§24. Simulation Study of Non-Diffusive Plasma Transport with Three Dimensional Particle Code

Hasegawa, H., Ishiguro, S.

Recently, non-diffusive (i.e., convective) plasma transport from the edge of core plasma to the first wall in magnetic confinement fusion devices[1)] is thought to be brought by intermittent filamentary coherent plasma structures "blobs" in scrape-off layer (SOL)[2)]. Although many theoretical and numerical studies about blob dynamics have been performed on the basis of two-dimensional reduced fluid models[3)], closure of parallel current and kinetic effects (e.g., sheath formation between a SOL plasma and a divertor plate, velocity difference between electrons and ions, etc.) are treated under some assumptions and parameterization in such kind of macroscopic models. Thus, we have developed a three-dimensional electrostatic plasma particle simulation code with particle absorbing boundaries[4)] and studied kinetic dynamics on the blob propagation[5)].

In our previous studies, the simulation system was set as grad-B is uniform in the toroidal and poloidal directions. In SOL plasmas of real magnetic confinement devices, however, the direction of grad-B is different between the inside and the outside of torus. In this study, we have investigated the blob kinetic dynamics in the system where grad-B varies in the toroidal direction. In our present simulation, the x, y, and z directions correspond to the counter radial direction, the poloidal direction, and the toroidal direction. The external magnetic field $\boldsymbol{B}$ does not have the y component. The x and z components of $\boldsymbol{B}$ are given as

$$\frac{B_x}{B_0} = -\frac{L_x}{D}\left[\ln\left(\frac{3}{2}-\frac{x}{2L_x}\right)+\ln\left(\frac{3-\alpha}{2}-\frac{x}{2L_x}\right) - \ln\left(\frac{5}{4}\right)-\ln\left(\frac{5}{4}-\frac{\alpha}{2}\right)\right]\mathrm{sech}^2\left(\frac{z-L_z/2}{D}\right) \quad (1),$$

$$\frac{B_z}{B_0} = \frac{L_x}{3L_x - x}\left[1-\tanh\left(\frac{z-L_z/2}{D}\right)\right] + \frac{L_x}{(3-\alpha)L_x + x}\left[1+\tanh\left(\frac{z-L_z/2}{D}\right)\right] \quad (2).$$

Thus, the direction of grad-B at z = 0 is opposite to that at z = L_z and B_x at x = L_x / 2 is zero as shown in Fig. 1. Here, B_0 is the magnetic field strength at (x, z) = (L_x , 0) where L_x, L_y, and L_z are the system lengths in the each direction, and D is set as D = L_z / 16. Particle absorbing boundaries corresponding to divertor plates are placed in the both ends of z axis. A particle absorbing boundary corresponding to the first wall is also placed at x = 0. In the y direction, periodic boundary condition is applied. The system size $L_x \times L_y \times L_z$ is 64 $\Delta \times$ 64 $\Delta \times$ 512 Δ where Δ is the grid spacing. The blob is initially located as a column along the ambient magnetic field at around (x, y) = (L_x / 2, L_y / 2). The effective width of the blob in the poloidal cross-section is δ_b = 4 Δ. The ion-to-electron mass ratio is m_i / m_e = 100. The initial ion-to-electron temperature ratio is T_i / T_e = 0.25.

We then calculate 4 cases where the coefficient α which appears in eqs. (1) and (2), the external magnetic field strength Ω_i / ω_{pi}, the grid spacing Δ, the time step Δt, and the blob localization [z_{b0}, z_{b1}] are set as (α, Ω_i / ω_{pi}, Δ / ρ_s, $\Omega_i \Delta t$, [z_{b0} / L_z, z_{b1} / L_z]) = (1, 1, 0.97, 2.42 x 10^{-3}, [0, 1]) [Fig. 1 (a); |$\boldsymbol{B}$| at (x, z) = (L_x / 2, 0) is equal to that at (x, z) = (L_x / 2, L_z)], (2, 0.5, 0.48, 1.21 x 10^{-3}, [0, 1]) [Fig. 1 (b); |$\boldsymbol{B}$| at z = 0 is smaller than that at z = L_z], (2, 0.5, 0.48, 1.21 x 10^{-3}, [0, 0.5]) [Fig. 1 (c); a blob is localized in the low-field side.], and (2, 0.5, 0.48, 1.21 x 10^{-3}, [0.5, 1]) [Fig. 1 (d); a blob is localized in the high-field side.], respectively. Here, Ω_i is the cyclotron frequency at (x, z) = (L_x, 0), ω_{pi} is the ion plasma frequency in the background plasma, ρ_s is defined as ρ_s = c_s / Ω_i, and c_s is the ion acoustic speed defined by c_s = $(T_e / m_i)^{1/2}$. In the case of Fig. 1 (a), the blob almost stays at initial position. In the case of Fig. 1 (b), the blob is torn across the magnetic field line. In the case of Fig. 1 (c), the blob propagates to the first wall ordinarily. In the case of Fig. 1 (d), the blob moves to the core. In each case, we also observe potential and particle flow structures different from those shown in our previous studies.

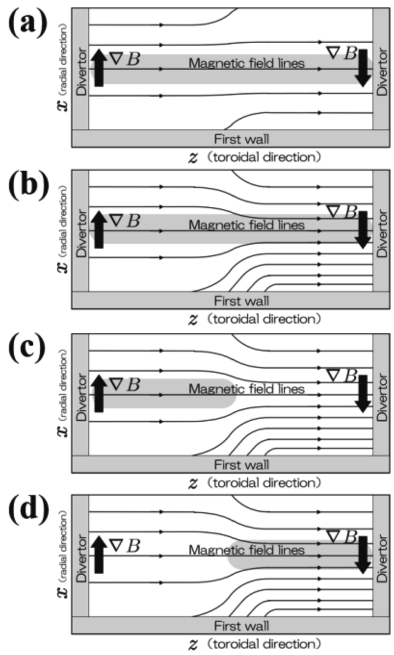

Fig. 1. Schematic diagrams of magnetic field configuration and initial location of a blob.

1) Umansky, M. V. et al.: Phys. Plasmas **5** (1998) 3373.
2) Krasheninnikov, S. I.: Phys. Lett. A **283** (2001) 368.
3) Krasheninnikov, S. I. et al.: J. Plasma Phys. **74** (2008) 679 and references therein.
4) Ishiguro, S. and Hasegawa, H.: J. Plasma Phys. **72** (2006) 1233.
5) Hasegawa, H. and Ishiguro, S.: Plasma Fusion Res. **7** (2012) 2401060.